Lawrence Berkeley National Laboratory
Recent Work

Title
Absolute calibration of GafChromic film for very high flux laser driven ion beams.

Permalink
https://escholarship.org/uc/item/15m6d4hm

Journal
The Review of scientific instruments, 90(5)

ISSN
0034-6748

Authors
Bin, JH
Ji, Q
Seidl, PA
et al.

Publication Date
2019-05-01

DOI
10.1063/1.5086822

Peer reviewed

Absolute calibration of GafChromic film for very high flux laser driven ion beams

J. H. Bin,[1,][*] Q. Ji,[1] P. A. Seidl,[1] D. Raftrey,[1] S. Steinke,[1] A. Persaud,[1]
K. Nakamura,[1] A. Gonsalves,[1] W. P. Leemans,[1] and T. Schenkel[1]

[1]*Lawrence Berkeley National Laboratory, University of California, Berkeley, California 94720, USA*
(Dated: March 24, 2019)

We report on the calibration of GafChromic HD-v2 radiochromic film in the extremely high dose regime up to 100 kGy together with very high dose rates up to 7×10^{11}Gy/s. The absolute calibration was done with nanosecond ion bunches at the Neutralized Drift Compression Experiment II (NDCX-II) particle accelerator at Lawrence Berkeley National Laboratory (LBNL) and covers a broad dose dynamic range over three orders of magnitude. We then applied the resulting calibration curve to calibrate a laser driven ion experiment performed on the BELLA petawatt laser facility at LBNL. Here, we reconstructed the spatial and energy resolved distribution of the laser-accelerated proton beams. The resulting proton distribution is in fair agreement with the spectrum that was measured with a Thomson spectrometer in combination with a microchannel plate (MCP) detector.

Following pioneering works [1–4], laser driven ion acceleration has evolved rapidly in recent years [5–8] and production of high energetic proton beams with energies up to nearly 100 MeV proton beams have been demonstrated [9, 10]. Tremendous progress has been achieved in the optimization of those ion beams towards high ion energy, small beam divergence and high ion yield and this can now enable a range of potential applications [5, 11–18]. These advances highlight the need for accurate diagnostics and also pose new diagnostics challenges, for example, under conditions of extremely high ion doses and dose rates.

GafChromic radiochromic film (RCF) has been used as a standard diagnostic ever since the first reports on MeV scale laser driven proton beams [1, 3, 4]. Calibrations for proton energy deposition have been reported for various RCF types [19–22]. However, for pulsed ion beams driven by relativistic laser pulses, the single shot dose can reach extreme high doses exceeding kGy and dose rates in excess of 10^{11}Gy/s. Absolute calibrations of the widely used versions of GafChromic RCF are currently lacking for the very high doses and dose rates present in laser-plasma driven ion acceleration experiments.

In this letter, we report on the calibration of the latest generation of RCF (i.e., HD-v2) over a large dose range from 100 to $\sim$100 kGy. In particular, this calibration is done with nanosecond pulsed ion bunches which deliver relevant radiation doses with very high dose rates up to 7×10^{11}Gy/s. This is in contrast to earlier experiments that applied more widely available continuous wave (CW) ion beams or low intensity ion pulses from conventional ion accelerators with irradiation times of milliseconds to seconds. The response functions of HD-v2 RCF were measured for RGB and grayscale channels. Saturation in the red channel was observed for doses beyond 10 kGy, while the response on the grayscale had reasonable sensitivity across the whole measured dose

range. We thus obtained our calibration using the response function of the grayscale using lease-squares fits. Furthermore, the calibration curve is applied to reconstruct the spatial and energy resolved distribution of a laser driven proton beam. We used Titanium foils of few μm thickness as laser targets and RCF in a stack configuration as the detector. The results were validated by a simultaneous measurement of the proton spectrum measured with a typical Thomson spectrometer for species and energy analysis in combination with a microchannel plate (MCP) detector.
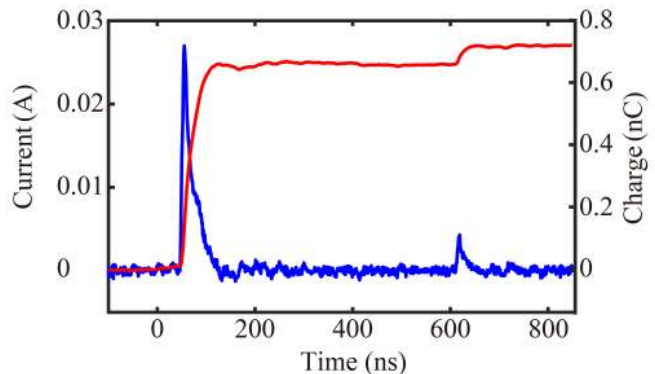

FIG. 1: (color online). Example of a proton pulse (1 MeV) from NDCX-II with current profile (blue) and integrated charge (red) from a fast Faraday cup. The peak at 620 ns is from H_2^+ ions. The proton pulse lengths was 10.12±1.29 ns (FWHM).

The calibration of HD-v2 films was performed at the Neutralized Drift Compression Experiment II (NDCX-II) particle accelerator at Lawrence Berkeley National Laboratory (LBNL) [23–25]. NDCX-II can deliver short helium and now also proton pulses with a pulse duration of 2 to 10 ns (full-width at half-maximum, FWHM), as shown in Fig. 1.

The energy of ion pulses from NDCX-II was measured to be 1.06±0.015 MeV [26]. As shown in Fig. 2, a scintillator was located at the focal plane of the proton
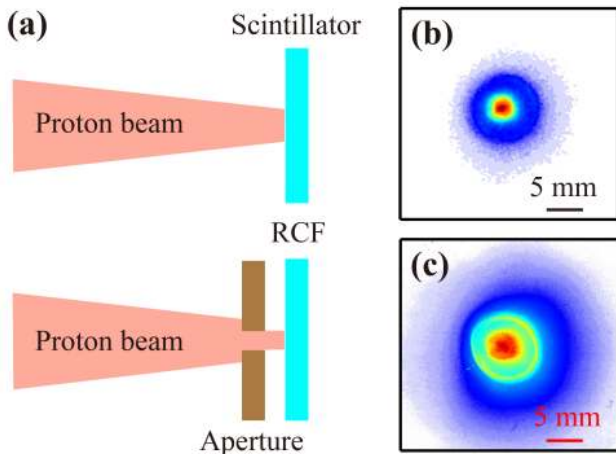
[*]jianhuibin@lbl.gov

FIG. 2: (color online). (a) Schematic of the experimental setup at NDCX-II. A scintillator was placed at the focal plane of the proton beam and a gated intensified CCD camera was used to capture the light emitted from the scintillator when struck by the proton bunch. RCF HD-v2 films were then located in the same location, and were irradiated by either an apertured proton beam (2 mm diameter) or the full beam (2.7 mm diameter). Examples of the dose distributions are shown in (b) and (c) for the full beam measured in situ with the scintillator (b) and by RCF ex situ (c).

beam, in where the full beam profile and flux were monitored by an 8-bit gated intensified CCD camera that was cross-calibrated to a removable fast Faraday cup. Subsequently, the HD-v2 films were placed in the same location and were irradiated under normal incidence. The flux was tuned in single proton bunches from $5.3\times10^{10}/cm^2$ to $2.4\times10^{11}/cm^2$ by adjusting the final solenoid magnets to control the convergence of the beam on the target. Single or multiple exposures were applied to HD-v2 films, yielding peak doses ranged from 650 Gy to $\sim$80 kGy. The dose is calculated by converting the total deposited energy of the incident proton beam within a given area in the sensitive layer of HD-v2 film, and including a small contribution from H_2^+ ions at 620 ns, that is also visible in Fig. 1. The deposited energy of protons and H_2^+ ions was calculated with SRIM [27] and the actual flux is extracted with beam profile information from scintillator images.

After the irradiation, the HD-v2 films were stored at room temperature within a light-tight envelope for at least 48 hours to stabilize the readout [28]. The films were then scanned with an EPSON V600 scanner, with a resolution of 1000 dpi in transmission mode for both 48-bit RGB color and 16-bit grayscale. The scanner was calibrated with a transparent step wedge [29], to convert the raw data to optical density (OD). In a standard configuration, the RCF calibration is done with an apertured proton beam of 2 mm diameter. We define this as low-dynamic-range (LDR) mode, in which the mean values over a half mm diameter around the local maximum were extracted as the peak value for both RCF and scintillator

results.

Fig. 3 (a) shows the resulting dose response curves in RGB color and in grayscale for doses from 0.65 to 80 kGy. The response curve in the red channel had the highest sensitivity for doses up to 10 kGy, above which the response saturated (see Fig. 3 (b)). No saturation effect was observed in the green and blue channels but the blue channel was the least sensitive to the delivered dose. Interestingly, the sensitivity in the grayscale is similar to that in the green channel with very little difference. We then chose to use the grayscale for our calibration of films from laser-plasma accelerated proton pulses in a compromise between the sensitivity and saturation effects.
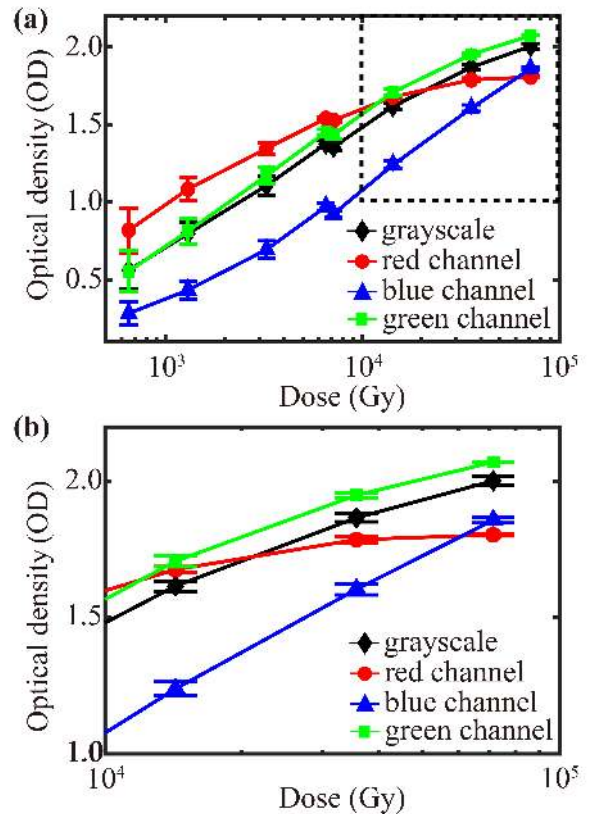

FIG. 3: (color online). (a) Dose response curves of separate RGB channels and the grayscale for GafChromic RCF HD-v2 with LDR mode. The vertical error bars indicate the standard deviation for each dose. (b) Magnified view of the black dotted zone of very high doses in (a).

In fact, the inhomogeneous distribution of the full proton beam with 2.7 mm FWHM diameter allows us to obtain a high-dynamic-range (HDR) dose response in a single shot, and thus we refer to the full beam irradiation as HDR mode. As shown in Fig. 2 (c), the dose response (OD) measured by the HD-v2 films presents similar asymmetry beam profile that measured by the scintillator. The measured OD can be spatially registered to a precise location in the scintillator images, i.e., to the delivered dose. Fig. 4 summarizes the results of

two HDR irradiations with peak doses of 550 and 6750 Gy, respectively (red circles). The LDR results (black circles) from Fig. 4 line up with the HDR data, confirming the consistence of the approach of using both irradiation modes. The full dynamic range of recorded doses extends to three orders of magnitudes. Dose versus OD over this full dynamic range is then fitted to a polynomial function $a \cdot OD + b \cdot OD^c$, similar to the approach in [30]. As shown in Fig. 4 by the black curve, which was fitted solely with our results (black and red circles), the best fit to our measurement is given by

$$\text{Dose(OD)} = 374.6 \cdot OD + 2557 \cdot OD^{3.085}, \quad (1)$$

When comparing our result to other calibration results in the lower dose range done with 10 MeV photons source [22] or pulsed proton beams [31], fair agreement is found, which further validates our calibration (see Fig. 4).
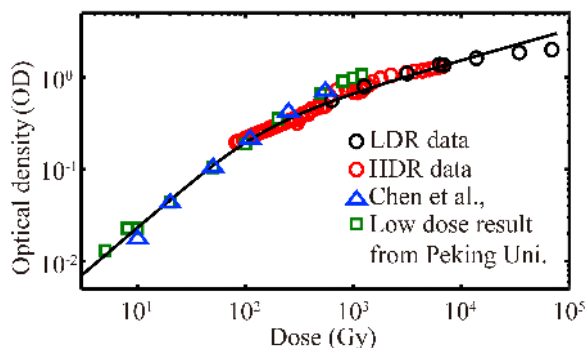

FIG. 4: (color online). Double logarithmic dose response curve in the grayscale for full dynamic range of 3 orders of magnitudes at NDCX-II, including both LDR (black circles) and HDR (red circles) results. The black curve shows the best fitted results with a polynomial function, which is well aligned with the previous calibration results (blue triangles and green squares) [22, 31] for doses below 1 kGy.

Note that, the current dynamic range from HDR mode is limited by the low bit-rate gated camera used for scintillator images, and could be further improved by replacing it with a higher bit-rate camera.

Though in our LDR and HDR modes, the applied dose rate varies from 8×10^9Gy/s to 7×10^{11}Gy/s, our results indicate that the dose rate effects only have a minor impact for the dose rate range applied in our experiment with the HD-V2 films. This is evidenced by the consistency of the LDR and HDR results in Fig. 4. Dose rate effects have been observed earlier in pulsed irradiation experiments with plastic scintillators [32, 33]. The unique beam characteristic (nanosecond pulse duration) of NDCX-II and of ion pulses from laser-plasma acceleration enable experimental studies of dose rate effect with various target materials in the very high dose rate regime of $\sim 10^{12}$Gy/s, and beyond with improved beam focusing.
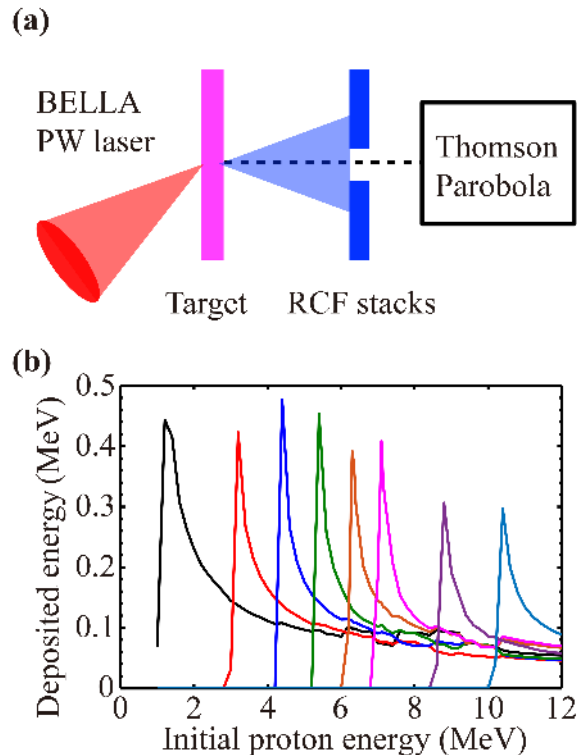

FIG. 5: (color online). (a) Schematic of the experimental setup for laser driven ion acceleration at BELLA centre. The BELLA PW laser pulse irradiates the target (a few μm thick Ti foils) at an oblique incidence angle of 45°. Protons are characterized with a Thomson parabola and RCF stacks. (b) RCF response functions for the stacks used in the experiments, which consists of 6 layers of HD-v2 followed by 2 layers of MD-v3. Here, the MD-v3 is calibrated by [34].

The new calibration is then applied to laser driven ion experiments performed at LBNL with the BELLA PW laser [35]. The laser system delivers 35 J with a wavelength centered at 815 nm. The 35 fs laser pulse was focused using a 13.5 m focal length off-axis parabolic mirror to a measured focal spot size of $\omega_0 \approx 52~\mu m$, where ω_0 is the beam radius at which the intensity drops to $1/e^2$ of the peak value. This yields to a peak intensity of $1.2 \times 10^{19}~W/cm^2$. The experimental setup is sketched in Fig. 5 (a). We irradiated titanium foils of few μm thickness at an angle of incidence of 45^0. A stack of RCF films was placed 10 cm downstream and parallel to the target foil to intercept and detect proton pulses. A layer of 15 μm Al foil was added in front of the RCFs to block the laser light as well as the heavy ions. Only protons with energy beyond 1 MeV can pass through the aluminum foil are recorded by the RCF stack. A small hole was bored through the RCF stack and allows ions to be detected further downstream by a Thomson Parabola (TP) spectrometer in combination with a microchannel plate (MCP) detector along the target normal direction. Note that, the optical system along with MCP used here is calibrated with an alpha source.
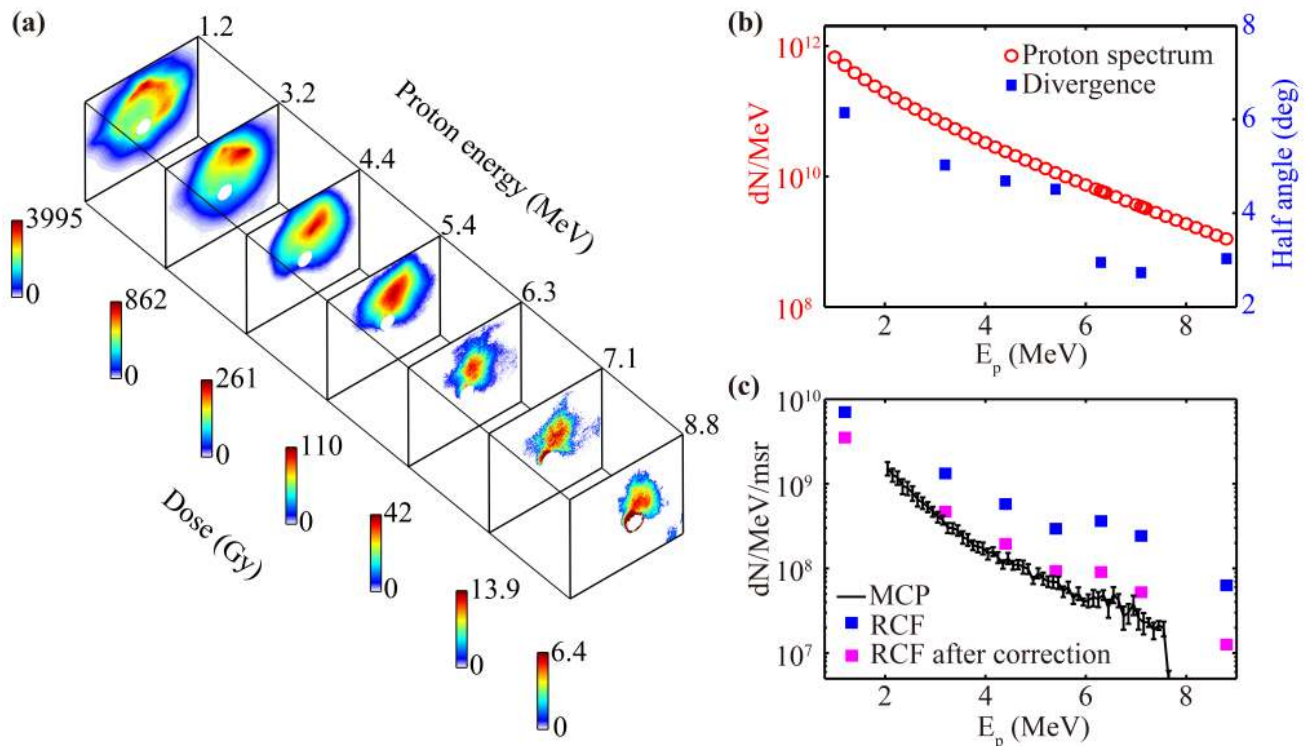
FIG. 6: (color online). (a) Three-dimensional proton spectrum for a 5 μm thick Titanium foil irradiated by the BELLA PW laser. Each slice presents a RCF layer measurement that was normalized to the local dose maximum. Above each slice the proton Bragg peak energy is given, and individual doses are indicated in the color bar. The corresponding proton beam divergence (blue squares) and reconstructed space-integrated proton spectra (red circles) are shown in (b). The comparison between the measurements from RCF stack (squares) and the TP spectrometer along with MCP (black curve) is shown in (c). The blue squares represent the derived energy distribution for the most energetic protons based on the reconstructed space-integrated proton spectra and the proton beam divergence, and magenta squares with correction for the detector position in the TP spectrometer.

The RCF films in stack configuration allows measurements of the proton beam profile at different energies. Fig. 5 (b) shows the response curves for a typical stack used in our experiments, where the deposited energy of protons inside the active layer of the RCFs was calculated using SRIM [27]. The response peak of each curves corresponds to an energy with most sensitivity (Bragg peak), which we refer as the proton Bragg peak energy for the corresponding RCF slice. The transverse cross section of the proton beam profile is then recorded at a given proton Bragg peak energy and can be used to determine the energy resolved beam divergence. Moreover, the proton spectrum can be reconstructed based on the calculated RCF response function. Assuming a certain function for proton spectrum, one could iteratively determine the parameters of such a function by comparing the calculated total energy loss for each RCF slices in the stack to the actual measurements. More information about the reconstruction algorithm can be found in [19–21]. Thus, the three-dimensional (3D) proton spectrum (including the spatial and energy resolved proton distributions) were determined with the RCF stack.

Fig. 6 shows an example of a reconstructed 3D proton spectrum. The proton beam profile recorded in each RCF slice is visualized in Fig. 6 (a) up to the 7th layers of the RCF stack, as no proton signal was observed at the 8th layer. We define the divergence by the half value of the FWHM of a Gaussian profile fitted to those measured beam profiles (Fig. 6 (b)). The space-integrated proton spectra dN/dE (see Fig. 6 (b)) is reconstructed with an assumed Boltzmann distribution for the protons $\frac{dN}{dE} = \frac{N_0}{E} exp(-\frac{E}{k_B T_e})$. The total number of protons was $N_0 = 1.17 \times 10^{12}$ and the hot electron temperature was $k_B T_e = 1.84$ MeV, as determined with a least-square fitting routine.

Finally, we compare our results to the measurement with the well-established TP spectrometer technique. The energy distribution $\frac{dN}{dE d\Omega}$ that is typically given by a TP spectrometer can be derived based on the divergence angles and the reconstructed space-integrated proton spectra dN/dE from RCF data. Fig. 6 (c) shows an energy distribution for the protons, derived from the same data in Fig. 6 (a). In order to compare our reconstructed proton distribution with the measurement from TP spectrometer, the exact location and the acceptance angle have to be taken into account. As seen

in Fig. 6 (a), even though the TP spectrometer was initially aligned along the target normal, a clear deflection of the intensity maximum of the protons pulses on the RCF stack of a few degrees from the target normal is observed for the most energetic protons (indicated by the hole position in the measurement). After including a small correction to account for this deflection and its effect on proton intensities at the downstream location of the detector in the TP spectrometer using a simple linear interpolation procedure, we find an updated proton energy distribution (Fig. 6 (c)) which we compare to the TP spectrometer data (black curve). Very close agreement between the RCF and TP spectrometer data is found when this correction is included.

In conclusion, we present a new absolute calibration measurement for the HD-v2 radiochromic film in an extremely high dose and dose rate approaching 100 kGy and 7×10^{11} Gy/s, respectively. The calibration was performed using the NDCX-II particle accelerator as a source of nanosecond proton pulses and covers a broad dose dynamic range over three orders of magnitude. During the calibration experiment, a novel HDR mode is employed, which increased the dynamic range of the measured dose range on a single shot basis. The sensitivity and saturation effects over the full dose range were measured in RGB and grayscale. The grayscale was the most suitable for large dose ranges and was used for the calibration. The calibration is further applied to laser accelerated ion beams and used for the 3D reconstruction of the proton spectrum. This procedure was then compared to the well-established TP spectrometer technique and good agreement between these two was found. This work is of particularly interest and beneficial for many applications, including the fundamental study of warm dense matter using high flux laser accelerated ion beams [36, 37], fast ignition [11], and generation of intense neutron pulses from laser-plasma accelerated ions [38]. Furthermore, material damage and processing studies with various target materials can benefit from the delivered extreme high dose rates from NDCX-II and from BELLA, a development that is being pursued at Berkeley Lab.

[1] R. A. Snavely, M. H. Key, S. P. Hatchett, T. E. Cowan, M. Roth, T. W. Phillips, M. A. Stoyer, E. A. Henry, T. C. Sangster, M. S. Singh, et al., Phys. Rev. Lett. **85**, 2945 (2000).

[2] E. L. Clark, K. Krushelnick, J. R. Davies, M. Zepf, M. Tatarakis, F. N. Beg, A. Machacek, P. A. Norreys, M. I. K. Santala, I. Watts, et al., Phys. Rev. Lett. **84**, 670 (2000).

[3] A. Maksimchuk, S. Gu, K. Flippo, D. Umstadter, and V. Y. Bychenkov, Phys. Rev. Lett. **84**, 4108 (2000).

[4] K. Krushelnick, E. L. Clark, M. Zepf, J. R. Davies, F. N. Beg, A. Machacek, M. I. K. Santala, M. Tatarakis, I. Watts, P. A. Norreys, et al., Physics of Plasmas (1994-present) **7** (2000).

[5] M. Borghesi, J. Fuchs, S. Bulanov, A. Mackinnon, P. Patel, and M. Roth, Fusion Science and Technology **49**, 412 (2006).

[6] H. Daido, M. Nishiuchi, and A. S. Pirozhkov, Reports on Progress in Physics **75**, 056401 (2012).

[7] A. Macchi, M. Borghesi, and M. Passoni, Rev. Mod. Phys. **85**, 751 (2013).

[8] J. Schreiber, P. R. Bolton, and K. Parodi, Review of Scientific Instruments **87**, 071101 (2016).

[9] F. Wagner, O. Deppert, C. Brabetz, P. Fiala, A. Kleinschmidt, P. Poth, V. A. Schanz, A. Tebartz, B. Zielbauer, M. Roth, et al., Phys. Rev. Lett. **116**, 205002 (2016).

[10] A. Higginson, R. Gray, M. King, R. Dance, S. Williamson, N. Butler, R. Wilson, R. Capdessus, C. Armstrong, J. Green, et al., Nature communications **9**, 724 (2018).

[11] M. Roth, T. E. Cowan, M. H. Key, S. P. Hatchett, C. Brown, W. Fountain, J. Johnson, D. M. Pennington, R. A. Snavely, S. C. Wilks, et al., Phys. Rev. Lett. **86**, 436 (2001).

[12] K. Krushelnick, E. Clark, R. Allott, F. Beg, C. Danson, A. Machacek, V. Malka, Z. Najmudin, D. Neely, P. Norreys, et al., IEEE transactions on plasma science **28**, 1110 (2000).

[13] J. Cobble, R. Johnson, T. Cowan, N. Renard-Le Galloudec, and M. Allen, Journal of applied physics **92**, 1775 (2002).

[14] D. Habs, T. Tajima, J. Schreiber, C. Barty, M. Fujiwara, and P. Thirolf, The European Physical Journal D **55**, 279 (2009).

[15] J. Bin, K. Allinger, W. Assmann, G. Dollinger, G. A. Drexler, A. A. Friedl, D. Habs, P. Hilz, R. Hoerlein, N. Humble, et al., Applied Physics Letters **101**, 243701 (2012).

[16] S. V. Bulanov, J. J. Wilkens, T. Z. Esirkepov, G. Korn, G. Kraft, S. D. Kraft, M. Molls, and V. S. Khoroshkov, Physics-Uspekhi **57**, 1149 (2014).

[17] B. Hidding, O. Karger, T. Königstein, G. Pretzler, G. Manahan, P. McKenna, R. Gray, R. Wilson, S. Wiggins, G. Welsh, et al., Scientific reports **7**, 42354 (2017).

[18] M. Barberio, M. Sciscìo, S. Vallières, F. Cardelli, S. Chen, G. Famulari, T. Gangolf, G. Revet, A. Schiavi, M. Sen-

zacqua, et al., Nature communications **9**, 372 (2018).

[19] D. S. Hey, M. H. Key, A. J. Mackinnon, A. G. MacPhee, P. K. Patel, R. R. Freeman, L. D. Van Woerkom, and C. M. Castaneda, Review of Scientific Instruments **79**, 053501 (2008).

[20] F. Nürnberg, M. Schollmeier, E. Brambrink, A. Blažević, D. C. Carroll, K. Flippo, D. C. Gautier, M. Geissel, K. Harres, B. M. Hegelich, et al., Review of Scientific Instruments **80**, 033301 (2009).

[21] M. Schollmeier, M. Geissel, A. B. Sefkow, and K. A. Flippo, Review of Scientific Instruments **85**, 043305 (2014).

[22] S. N. Chen, M. Gauthier, M. Bazalova-Carter, S. Bolanos, S. Glenzer, R. Riquier, G. Revet, P. Antici, A. Morabito, A. Propp, et al., Review of Scientific Instruments **87**, 073301 (2016).

[23] W. Waldron, W. Abraham, D. Arbelaez, A. Friedman, J. Galvin, E. Gilson, W. Greenway, D. Grote, J.-Y. Jung, J. Kwan, et al., Nuclear Instruments and Methods in Physics Research Section A: Accelerators, Spectrometers, Detectors and Associated Equipment **733**, 226 (2014), 19th International Symposium on Heavy Ion Inertial Fusion.

[24] P. A. Seidl, A. Persaud, W. L. Waldron, J. J. Barnard, R. C. Davidson, A. Friedman, E. P. Gilson, W. G. Greenway, D. P. Grote, I. D. Kaganovich, et al., Nuclear Instruments and Methods in Physics Research Section A: Accelerators, Spectrometers, Detectors and Associated Equipment **800**, 98 (2015).

[25] P. Seidl, J. Barnard, E. Feinberg, A. Friedman, E. Gilson, D. Grote, Q. Ji, I. Kaganovich, B. Ludewigt, A. Persaud, et al., Laser and Particle Beams **35**, 373 (2017).

[26] F. Treffert, Q. Ji, P. Seidl, A. Persaud, B. Ludewigt, J. Barnard, A. Friedman, D. Grote, E. Gilson, I. Kaganovich, et al., Review of Scientific Instruments **89**, 103302 (2018).

[27] J. F. Ziegler, M. D. Ziegler, and J. P. Biersack, Nuclear Instruments and Methods in Physics Research Section B:

Beam Interactions with Materials and Atoms **268**, 1818 (2010).

[28] W. L. McLaughlin, C. Yun-Dong, C. G. Soares, A. Miller, G. Van Dyk, and D. F. Lewis, Nuclear Instruments and Methods in Physics Research Section A: Accelerators, Spectrometers, Detectors and Associated Equipment **302**, 165 (1991).

[29] Transparent step wedge #T4110, Stouffer Graphic Arts, Mishawaka, IN 46544, USA, `http://www.stouffer.net/`.

[30] S. Devic, J. Seuntjens, G. Hegyi, E. B. Podgorsak, C. G. Soares, A. S. Kirov, I. Ali, J. F. Williamson, and A. Elizondo, Medical physics **31**, 2392 (2004).

[31] Peking University, private communication.

[32] M. M. Hamada, P. R. Rela, F. E. da Costa, and C. H. de Mesquita, Nuclear Instruments and Methods in Physics Research Section A: Accelerators, Spectrometers, Detectors and Associated Equipment **422**, 148 (1999).

[33] M. Zimmer, *Neutralized drift compression for short and intense ion pulses*, Master thesis, TU Darmstadt (2016).

[34] J. P. Chung, S. W. Oh, Y. M. Seong, K. J. Chun, and H.-T. Chung, Physica Medica **32**, 368 (2016).

[35] K. Nakamura, H. Mao, A. J. Gonsalves, H. Vincenti, D. E. Mittelberger, J. Daniels, A. Magana, C. Toth, and W. P. Leemans, IEEE Journal of Quantum Electronics **53**, 1 (2017).

[36] P. K. Patel, A. J. Mackinnon, M. H. Key, T. E. Cowan, M. E. Foord, M. Allen, D. F. Price, H. Ruhl, P. T. Springer, and R. Stephens, Phys. Rev. Lett. **91**, 125004 (2003).

[37] G. M. Dyer, A. C. Bernstein, B. I. Cho, J. Osterholz, W. Grigsby, A. Dalton, R. Shepherd, Y. Ping, H. Chen, K. Widmann, et al., Phys. Rev. Lett. **101**, 015002 (2008).

[38] M. Roth, D. Jung, K. Falk, N. Guler, O. Deppert, M. Devlin, A. Favalli, J. Fernandez, D. Gautier, M. Geissel, et al., Phys. Rev. Lett. **110**, 044802 (2013).